Low-Intensity High-Temperature (LIHT) Solar Cells for Venus Atmosphere

Jonathan Grandidier, Alexander P. Kirk, Mark L. Osowski, Pawan K. Gogna, Shizhao Fan, Minjoo L. Lee, Margaret A. Stevens, Phillip Jahelka, Giulia Tagliabue, Harry A. Atwater, and James A. Cutts

***Abstract*—Low-intensity high-temperature solar cells that operate effectively in the atmosphere of Venus at various altitudes and also survive on the 465 °C surface of Venus are being developed. Thermal stability, high-temperature current–voltage (*I–V*), and external quantum efficiency measurements on GaInP/GaAs double-junction solar cells are presented. Solar-cell modeling under the atmospheric conditions of Venus is used to design the optimum solar-cell structure.**

***Index Terms*—High-temperature photovoltaics, multi-junction solar cells, Venus exploration missions.**

I. Introduction

VENUS exploration missions have been mostly limited to orbital and short-duration surface missions. Venus orbital missions were implemented with state-of-practice (SOP) solar cells as the Venus orbital environmental conditions are benign and similar to that of the earth orbital missions. Short-duration Venus mid- to surface-level missions of a few hours were implemented using SOP primary batteries enclosed in an environmental chamber equipped with a complex thermal management subsystem. These Venus mid- to surface-level missions did not consider the use of solar power systems because SOP solar cells cannot function in severe Venus surface environments. This study is focused on the development of solar power system technologies required for mid/low-altitude Venus exploration missions. Venus variable-altitude (mid- to surface-level) missions, which employ, for example, altitude-cycling balloons that observe both the atmosphere and the surface [1], require solar power systems that can operate at 200–350 °C for several months, survive the 465 °C surface temperature for a short duration, generate power under 100–300 W/m^2 solar irradiance conditions, and survive in a corrosive atmosphere. The GaInP/GaAs double-junction (2 J) solar cell presented here may, with suitable encapsulation, be capable of operation in the Venus atmosphere and survive in the high-temperature conditions on the surface of Venus [2], [3]. In this study, an overview of Venus atmospheric conditions is presented with a focus on the solar spectra at different altitudes as they were measured by the Venera 11 [4] and Venera 13 [5] descent probes. This is followed by a description of the structure of a solar cell that can operate on Venus. Results of the 2 J cell performance before and after heating to 465 °C and under high-temperature operation (300 °C, which corresponds to an altitude of 21 km on Venus) are presented. Current–voltage (*I–V*) and external quantum efficiency (EQE) measurements weighted by the Venus solar spectrum at an altitude of 21 km are presented to predict the performance of the solar cell under Venus conditions. Finally, solar-cell modeling is used to help guide future improvements to the solar-cell design for improved performance under realistic Venus atmospheric conditions.

Manuscript received May 15, 2018; revised August 28, 2018; accepted September 9, 2018. This work was supported by the National Aeronautics and Space Administration (NASA) through the ROSES16 HOTTech Program in the Science Mission Directorate. The work of M. A. Stevens was supported by the NASA Space Technology Research Fellowship through Award NNX15AQ79H. *(Corresponding author: Jonathan Grandidier.)*

J. Grandidier, P. K. Gogna, M. A. Stevens, and J. A. Cutts are with the Jet Propulsion Laboratory, California Institute of Technology, Pasadena, CA 91109 USA (e-mail: jonathan.grandidier@jpl.nasa.gov; pawan.k.gogna@jpl.nasa.gov; margaret.stevens@tufts.edu; james.a.cutts@jpl.nasa.gov).

A. P. Kirk and M. L. Osowski are with MicroLink Devices Inc., Niles, IL 60714 USA (e-mail: akirk@mldevices.com; mosowski@mldevices.com).

S. Fan and M. L. Lee are with the University of Illinois at Urbana-Champaign, Urbana, IL 61801 USA (e-mail: shizhao@illinois.edu; mllee@illinois.edu).

P. Jahelka, G. Tagliabue, and H. A. Atwater are with the , Thomas J. Watson Laboratory of Applied Physics, California Institute of Technology, Pasadena, CA 91125 USA (e-mail: pjahelka@caltech.edu; giuliat@caltech.edu; haa@caltech.edu).

Color versions of one or more of the figures in this paper are available online at http://ieeexplore.ieee.org.

Digital Object Identifier 10.1109/JPHOTOV.2018.2871333

II. Venus Atmospheric Conditions

Venus atmospheric conditions are very different from those on earth. Venus is a hot and dry planet. The 90-bar atmosphere is composed primarily of carbon dioxide (CO_2) but also includes trace amounts of nitrogen (N_2), water vapor (H_2O), sulfur dioxide, carbonyl sulfate, hydrochloric acid, hydrofluoric acid, and sulfuric acid (H_2SO_4). Clouds cover the entire planet in three layers (upper, middle, and lower) between 48 and 68 km altitude. H_2SO_4 is the principal constituent of the cloud particles. A thin haze layer extends above and below the main cloud decks.

The two Soviet descent probes, Venera 11 [4] and Venera 13 [5], measured the spectrally dependent downward solar radiation at altitudes between the surface and 62 km. Venera 11 entered the Venusian atmosphere at −14° latitude at 10:10 A.M. local solar time (solar zenith angle 17°) on December 25, 1978, whereas Venera 13 entered at −7.5° latitude at 9:27 A.M. local time (solar zenith angle 38°) on March 1, 1982 [6]. The solar intensity measured by Venera 11 was about 1.8 times higher than the solar intensity measured by Venera 13. The solar zenith angle changes the path length by about 20%. With an H_2SO_4 cloud optical depth of 25–40, that variation in path length ac-

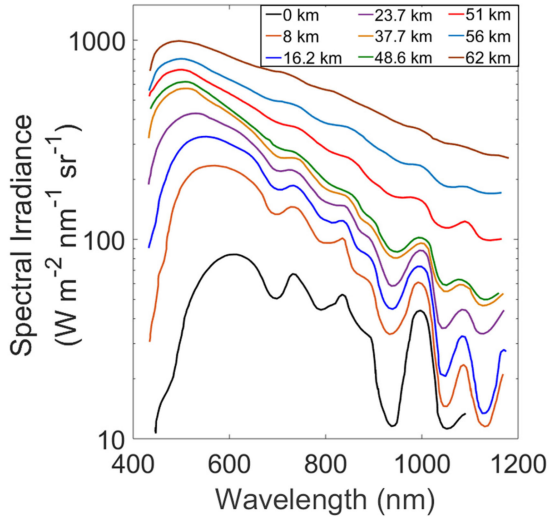

Fig. 1. Solar spectra of the downward-scattered solar radiation measured by the Venera 11 descent probe at various altitudes between 62 km and the surface of Venus.

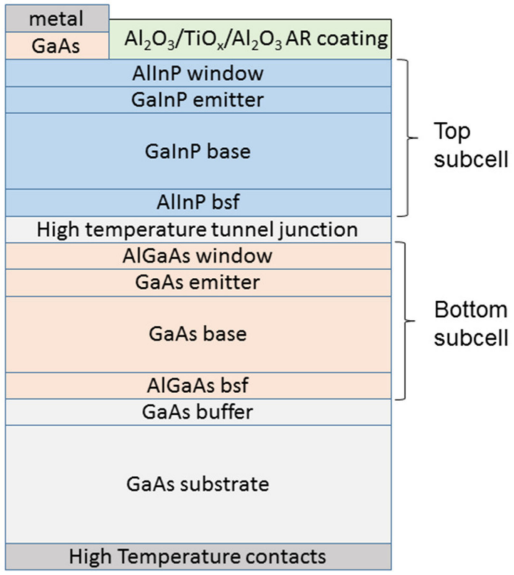

Fig. 2. Simplified cross-section schematic of a GaInP/GaAs 2 J solar cell designed for high-temperature operation.

counts for the large difference in solar intensity. This study uses data from Venera 11, as the measurements were taken closer to noon local time and are, therefore, closer to the highest solar intensity values that can be expected.

Fig. 1 shows the downward-scattered solar spectrum measured by the Venera 11 probe at various altitudes during its descent in the Venus atmosphere. Venus orbits the Sun at a distance of 0.72 astronomical unit (AU), and the solar intensity above the Venus atmosphere is ~2622 W/m^2, which is about twice the earth air mass 0 (AM0) extra-terrestrial solar intensity (~1366 W/m^2). However, sunlight intensity is significantly attenuated by scattering and absorption within the atmosphere of Venus. Within and below the main cloud deck, most of the solar radiation useful for power generation is scattered [7]. Direct solar radiation can be neglected at altitudes below 60 km [8]. Sunlight is nearly isotropic below the lower clouds, and the Lambertian distribution can be used to estimate the downward solar flux for a given altitude z as follows:

$$F_D(z) = I(z) \int_0^{\pi/2} \int_0^{2\pi} \cos\theta \sin\theta \, d\varphi \, d\theta \qquad (1)$$

where $I(z)$ is the solar flux per steradian, θ is the zenith angle, and φ is the azimuth angle. Solving (1), $F_D(z) = \pi I(z)$. $I(z)$ can be calculated by integrating the solar spectrum at a given altitude z over the whole wavelength range. At the surface of Venus ($z = 0$), where the temperature is 465 °C, the surface solar spectrum measured by Venera 11 and shown in Fig. 1 can be used to calculate $I(0) = 28.4$ W/m^2/sr. This corresponds to a downward flux of $F_D(0) = 89.4$ W/ m^2, which is only 3.4% of the solar intensity outside the Venus atmosphere. At an altitude of 21 km above the surface of Venus, where the temperature is 300 °C, the solar spectra measured by Venera 11 can be used to interpolate the Venus solar spectrum I(21 km) = 128.3 W/m^2/sr, which corresponds to a downward flux of F_D(21km) = 403.1 W/ m^2.

III. Solar-Cell Structure

A schematic diagram of the GaInP/GaAs solar cell layer design under development is shown in Fig. 2. This solar cell was initially designed for high-temperature terrestrial application under concentrated sunlight [9]. Modifications are needed to optimize the design for the Venus solar spectrum and temperature. The epitaxial structure employs the same GaInP top subcell that is found in standard triple-junction GaInP/GaInAs/Ge solar cells; however, the design does not contain a Ge subcell. This modification improves the high-temperature performance of the cells as the Ge subcell becomes ineffective at high temperatures [10], [11]. The solar cell has several features that make it suitable for the Venus environment. It has a tunnel junction that demonstrated stable operation at 400 °C [3]. It has contact electrodes that are thermally stable at 465 °C for up to 24 h, as presented in Section IV. It has an $Al_2O_3/TiO_x/Al_2O_3$ antireflection coating (ARC) that may help provide a limited amount of protection to the top grid metal electrode against the corrosive Venus environment.

IV. Survivability at High Temperature

Heat-exposure tests were performed on the GaInP/GaAs 2 J solar cells with temperatures up to 465 °C. The cells incorporated a high-temperature metal stack consisting of barrier metals and a conductive Ag layer. The barrier metals and their thickness were optimized for high-temperature operation. The *I–V* behavior was measured at 25 °C under simulated AM0 illumination before and after heating on a hot plate. The high-temperature soak was performed for up to 1 week in a high-vacuum chamber (10^{-7} torr). Fig. 3 shows the two experimental conditions that mimic the Venus environment at two different altitudes. One was at 300 °C, which corresponds to the temperature at an altitude of 21 km, and the other was at 465 °C, which corresponds to the surface temperature. Solar-cell efficiency measured under

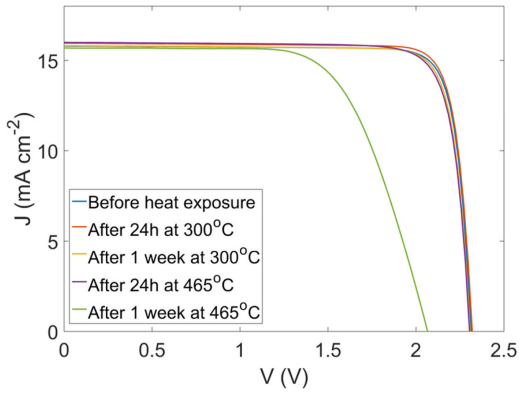

Fig. 3. *I–V* response (AM0 spectrum) of a GaInP/GaAs 2 J solar cell with a high-temperature grid metal and an $Al_2O_3/TiO_x/Al_2O_3$ ARC before and after heating four different solar cells on a 300 and 465 °C hot plate for 24 h and 1 week in a high-vacuum chamber.

the AM0 solar spectrum was 22.7%. Results showed no degradation in cell performance after exposure at 300 °C for up to 1 week. No degradation in cell performance was observed after 24 h of exposure at 465 °C. After 1 week of exposure at 465 °C, the cells experienced a higher series resistance and a large reduction in open-circuit voltage V_{oc} with dim electroluminescence (not shown), which indicated material dominated by parasitic non-radiative recombination. This degradation may be due to the diffusion of metal into the GaInP subcell caused by the extreme temperature exposure [12]. Despite the degradation, the solar cell yielded a post-heat exposure efficiency of 15.6% under the AM0 spectrum at 25 °C. The preliminary findings indicate that the cells could be robust at high temperatures, when kept in an inert environment free from O_2 gas and H_2O vapor. A longer duration and a more extensive testing and evaluation are required to better understand the performance of the cells in a realistic (corrosive) Venus atmosphere.

V. Solar-Cell Characterization

High-temperature *I–V* and EQE measurements were performed on the solar cell using a steel plate with two heaters that can raise the temperature up to 500 °C. The solar cell rested on the steel plate and was mechanically held with steel bars on the lateral busbar of the solar cell. The mechanical holder was designed this way to avoid the use of paste that could outgas at high temperatures. To prevent any reaction with the surrounding environment, the setup was mounted inside a bell jar purged with N_2 gas. For characterization, the solar cell was illuminated using a ScienceTech solar simulator and an EQE measurement device through a quartz window. Fig. 4(a) shows the *I–V* measurements of the solar cell between 25 and 300 °C.

For a given subcell, the open-circuit voltage V_{oc} is [11] given by

$$V_{oc} = \frac{nkT}{q} \ln\left(\frac{J_{sc}}{J_0}\right) \tag{2}$$

where n is the diode ideality factor, k is the Boltzmann constant, T is the temperature, q is the electron charge, J_{sc} is the short-circuit current density, and J_0 is the reverse saturation current

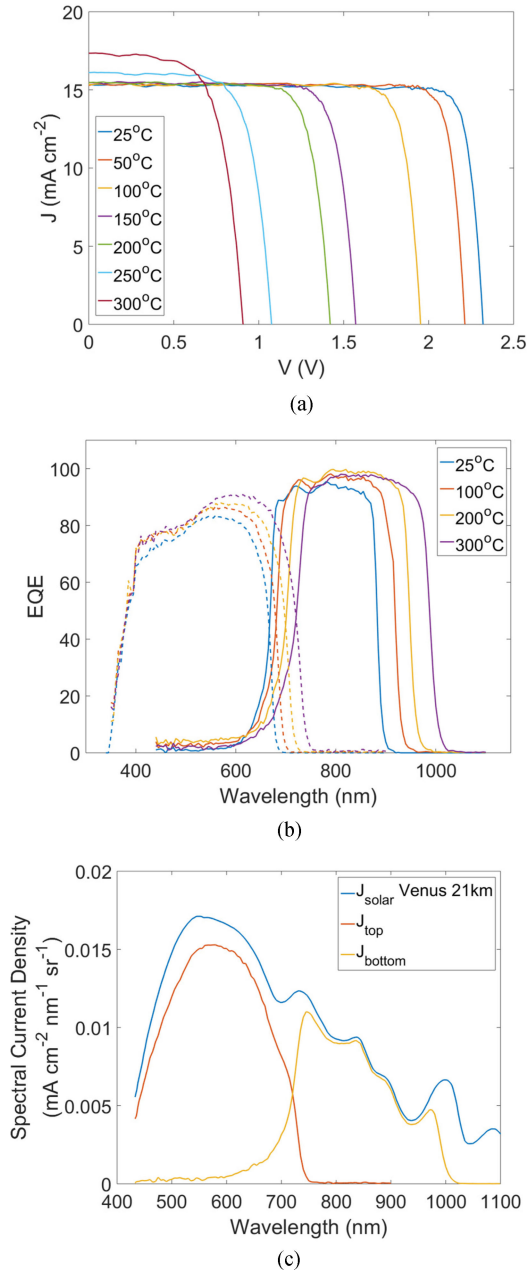

Fig. 4. (a) Variable-temperature *I–V* measurements of a GaInP/GaAs 2 J solar cell between 25 and 300 °C using an AM0 solar simulator. (b) Variable-temperature EQE measurements of a GaInP (dash line)/GaAs (solid line) 2 J solar cell between 25 and 300 °C. (c) Calculated current density in the GaInP (3.90 mA/cm^2) and GaAs (2.42 mA/cm^2) subcells for the 300 °C EQE data using the Venus solar spectrum at an altitude of 21 km, where the temperature is 300 °C. The solar cell has not yet been optimized for the Venus spectrum.

density. As expected, the temperature increase affects V_{oc}, which decreases from 2.32 V at 25 °C to 0.91 V at 300 °C. As shown in Fig. 4(a), J_{sc} remains stable at ∼15.5 mA/cm^2 for up to 200 °C and, then, rises to 17.31 mA/cm^2 at 300 °C. The fill factor FF decreases from 0.88 to 0.67 between 25 and 300 °C.

EQE measurements from the same device are depicted in Fig. 4(b). At 25 °C, the measured bandgap is 1.85 eV (∼670 nm) for the top junction and 1.39 eV (∼890 nm) for the bottom junction. At 300 °C, the bandgaps shift to 1.68 eV (∼740 nm) for

the top junction and 1.24 eV (∼1000 nm) for the bottom junction. The pressure in the atmosphere of Venus can reach almost 100 bars. The effect on the semiconductor bandgaps is not significant at this pressure [13]. The EQE measurement at 25 °C when weighted by the AM0 solar spectrum gives 16.64 mA/cm^2 for the top subcell and 15.60 mA/cm^2 for the bottom subcell. The two subcells generate almost the same amount of current with the bottom subcell being slightly current-limiting. This result is consistent with the short-circuit current measurement of 15.66 mA/cm^2 at 25 °C shown in Fig. 4(a). As the temperature increases, the EQE improves in the GaInP subcell. An ordered GaInP possesses a large number of shallow traps that reduce the EQE compared with a disordered material at room temperature [14]. As the temperature increases, carriers gain sufficient thermal energy to escape these traps, which dramatically increases the EQE of the ordered material. The simulations presented in Section VI do not fully model these shallow traps, which is why the EQE only shows a modest increase with temperature because of shifting band alignments and index of refraction mismatches. The experimental EQE of a disordered GaInP will only show modest changes in the EQE similar to our model. In order to evaluate the effects of the Venus solar spectrum on the solar cell, the EQE measurement was weighted by the Venus solar spectrum. The highest measured temperature presented here is 300 °C. The Venus solar spectrum data for an altitude of 21 km were interpolated from the solar spectrum curves measured at various altitudes by the Venera 11 descent probe [5]. Fig. 4(c) shows the 300 °C EQE measurement weighted by the Venus solar spectrum at 21 km. This corresponds to the spectral current density as described in the literature [15], [16]. The current density generated by the top subcell is 3.48 mA/cm^2/sr, while the current density generated by the bottom subcell is 2.22 mA/cm^2/sr. This makes the bottom subcell current-limiting; therefore, to operate optimally, the subcells need to be adjusted. The most straightforward way to optimize the solar cell is to thin the top subcell in order to generate the same amount of current in both subcells. After adjustment, both subcells would give a current density of $\sim(3.48 + 2.22)/2 = 2.85$ mA/cm^2/sr. The power conversion efficiency of the solar cell is defined as follows:

$$\eta = \frac{FFJ_{\rm sc}V_{\rm oc}}{P_{\rm in}} \tag{3}$$

where $P_{\rm in}$ is the incident solar input power. At 300 °C and 21 km, the model presented in Section VI was used to estimate the FF and $V_{\rm oc}$. The calculated FF was 0.61, and the $V_{\rm oc}$ was 0.85 V. Integrating the Venus solar spectrum at 21 km over the wavelength range measured by Venera 11, the calculated solar irradiance $P_{\rm in}$ is 128 W/m^2/sr. Therefore, the estimated efficiency of the adjusted solar cell is 11.5%, and the estimated power density is 14.8 W/m^2/sr. For comparison, the measured efficiency of the preliminary Gen1 solar cell at 25 °C under the standard AM0 solar spectrum is 22.7%. As described earlier, $F_D(21\text{ km}) = 403.1$ W/m^2. The average absorption of light as a function of the incidence angle normalized by the orthogonal incidence angle [17] averages to 0.68 for a typical commercial solar cell. Accounting for both the total downward solar flux and incidence angle gives a power density of 31.6 W/m^2 and an efficiency of 7.8% at an altitude of 21 km and a temperature of 300 °C. Because of scattering and atmospheric conditions, the upward solar flux at Venus is very important and can be approximated, below the clouds, by $F_U(z) = F_D(z) - 40$ W/m^2 [18]. Taking advantage of both downward and upward flux could increase the power density up to 69 W/m^2 at an altitude of 21 km and a temperature of 300 °C. Given the nearly isotropic nature of the solar flux below an altitude of 60 km, the solar cells could be oriented at any angle. For a Venus balloon mission [19], it may be more practical to have the solar cells oriented vertically.

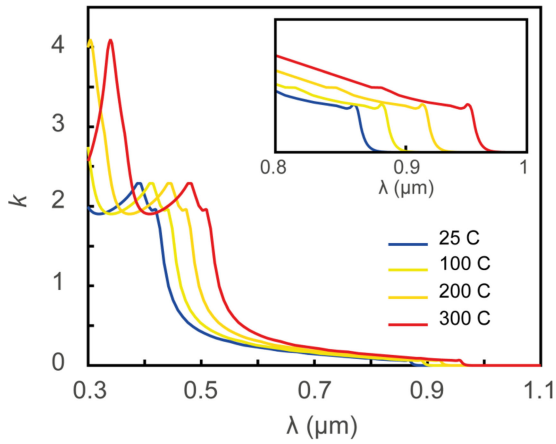

Fig. 5. GaAs temperature-dependent extinction coefficient k. The inset shows a zoomed-in view of the onset of inter-band transitions.

VI. High-Temperature Solar-Cell Modeling

A. Temperature Dependence of a Low-Intensity High-Temperature Solar Cell

It is essential to model the temperature-dependent optical and electronic properties in order to establish a functional model of a high-temperature multi-junction solar cell. The initial design is a 2 J solar cell with a GaInP top subcell and a GaAs bottom subcell. In addition, AlInP and AlGaAs are used as the window and back surface field layers for the top and bottom subcell, respectively. The temperature dependence of the material bandgap $E_g(T)$ is described by the standard Varshni equation, given by

$$E_g(T) = E_g(0) - \frac{\alpha T^2}{\beta + T}. \tag{4}$$

For GaAs, $E_g(0\text{ K}) = 1.519$ eV, $\alpha = 5.405 \times 10^{-4}$eV/K, and $\beta = 204$K.

The extinction coefficient k describes the light-absorption properties of the material, and thus, it is one parameter that is required to correctly model the solar cell performance. In particular, the onset of absorption (i.e., $k > 0$) must coincide with the onset of inter-band transitions. Therefore, in order to model the high-temperature response of the subcells, the material's complex refractive index spectrum was shifted by an amount equal to the reduction in the material bandgap $\Delta E_g(T) = E_g(T_{nk}) - E_g(T)$, as shown in Fig. 5. The inset in Fig. 5 precisely illustrates the shift in the GaAs bandgap as the temperature increases. The validity of this approximation

is supported by experimental results in the literature [20], as well as by the good agreement between our modeling and the experimental data. In the case of GaInP, accurate refractive index data were not enough to correctly capture the spectrally resolved photocurrent generation of the top cell depicted in Fig. 4(b). The result improved when the quantum yield was reduced from 1 to 0.88. This reduced material performance can be attributed to an increased ordering of the grown material [14], [21], [22].

B. Computational Model and Low-Intensity High-Temperature Solar-Cell Design

Technology computer-aided design software Synopsys Sentaurus was used to create a computational model of the solar cell shown in Fig. 2. The transfer-matrix method [23], [24] was used to determine the optical generation profile across the cell stack. Furthermore, the modeling of the tunnel junction that connects the top and bottom cells required special consideration. In fact, the material database band-alignment values for degenerately doped AlGaAs and GaAs resulted in an incorrect electrical behavior of the junction. In particular, the mismatched band-alignment caused a large voltage loss to occur across the tunnel junction during operation. In order to avoid this problem, two fictitious materials were created (AlGaAs and GaAs), which have the same optical properties of the initial semiconductors but behave electrically as metals. This approximation is valid because of the degenerate doping of the tunnel junction materials. Overall, this approach ensures the correct generation of charge carriers in the bottom subcell while maintaining a good electrical connection between the two subcells. In order to validate our computational model, the performance of the solar cell was computed under AM0 illumination and compared with the experimental measurements presented in Section V. In particular, the EQE and the *I–V* response of the solar cell were modeled at 25, 100, 200, and 300 °C. While the GaAs subcell model agrees well with the experimental results, the GaInP subcell presents some minor discrepancies. This is expected from a material that has a variable bandgap energy and minority carrier lifetime via changes in the amount of alloy disorder [14].

The expected short-circuit current density under AM0 was calculated to be 15.3 mA/cm^2, which is in good agreement with the experimental value of 15.5 mA/cm^2. In terms of temperature-dependent behavior, our model was used to determine the *I–V* response of the solar cell under AM0 illumination. The modeled temperature-dependent open-circuit voltage V_{oc} was compared with the experimental results depicted in Fig. 4(a). The comparison is depicted in Fig. 6(a). This result is also in good agreement with values reported elsewhere on a similar structure [9]. This further confirms the validity of our computational model. The model was used to compute the performance of this multijunction solar cell under Venus solar illumination. In particular, the solar spectrum measurement from the Venera 11 mission [4] was used to compute the *I–V* response using the 21-km solar spectrum for a temperature of 300 °C. Further analysis of this result showed that the bottom cell is strongly current-limiting under Venus illumination conditions. Indeed, this observation is in agreement with predictions made based on the EQE measurement weighted by the Venus spectrum and depicted in Fig. 4(b). Our computational model was used to optimize the structure of the 2 J device and propose an optimized solar cell for the Venus atmosphere. The optimization was performed for 21 km and at 300 °C.

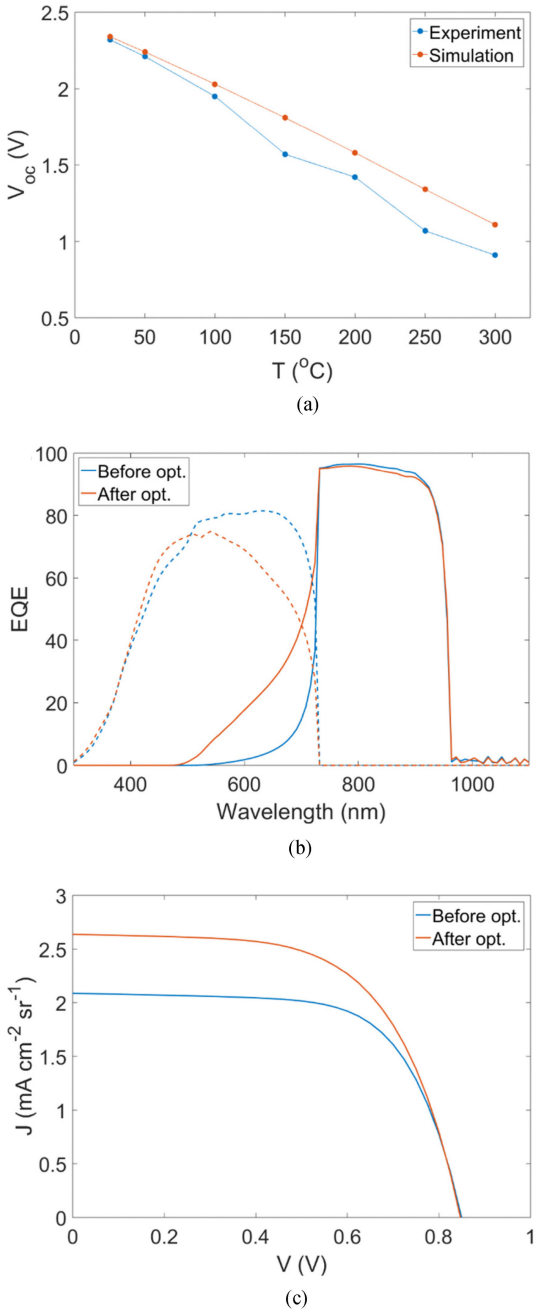

Fig. 6. (a) Comparison between the calculated $V_{oc}(T)$ and the measurement depicted in Fig. 4(a). (b) EQE of the top GaInP and bottom GaAs subcells in the optimized device. (c) *I–V* curve of the optimized Gen2 device versus the Gen1 device under the target condition of Venus irradiation at 21 km and 300 °C.

The solar-cell design was optimized by reducing the thickness of the GaInP base from 700 to 220 nm. This configuration results in the generation of a more uniform photocurrent from the two subcells. Fig. 6(b) shows the EQE before and after optimization. As depicted in Fig. 6(c), the optimized solar cell shows a 28.6% improvement in current density output from 2.1

to 2.7 mA/cm^2/sr. This value is in good agreement with the 2.85 mA/cm^2/sr calculated from the simplified optimization model proposed in Section V.

VII. Conclusion

GaInP/GaAs 2 J solar cells have shown a promising performance under high-temperature characterization with no degradation in the *I–V* response after up to 24 h of exposure to temperatures as high as 465 °C (a temperature typical of the surface of Venus). A duration of 24 h is significantly longer than the most successful lander, Venera 13, which survived for a mere 127 min back in 1982. At a given altitude (temperature and spectrum), an optimized 2 J solar cell is likely to be more efficient than a single-junction solar cell because of better photon energy management. The optimization would shift at different temperatures and altitudes, and we plan to investigate this sensitivity. Advanced solar-cell modeling has shown good agreement with experimental results and has been used to propose the optimum GaInP/GaAs 2 J solar-cell design for the 21-km altitude solar spectrum and 300 °C temperature. Measurements have shown that a power density of 37 W/m^2 may be attainable for GaInP/GaAs 2 J solar cells under the Venus solar spectrum at an altitude of 21 km and a temperature of 300 °C, provided that the solar cells and modules are properly encapsulated. This is encouraging for potential application in a future long-duration solar-powered mid- to surface-level Venus exploration mission. Work has been ongoing to optimize the grid metal electrodes for a better performance of the GaInP/GaAs 2 J solar cells after a longer duration (up to 1 month) exposure to a temperature of 465 °C.

Acknowledgment

The authors would like to thank D. Crisp for his contribution related to the Venus atmosphere and J. A. Schwartz for valuable discussions. The research was carried out at the Jet Propulsion Laboratory, California Institute of Technology, at MicroLink Devices Inc., at the California Institute of Technology, and at the University of Illinois at Urbana Champaign.

References

[1] M. de Jong, "Venus altitude cycling balloon," in *Proc. Venus Lab Technol. Workshop*, 2015.

[2] G. Landis and E. Haag, "Analysis of solar cell efficiency for Venus atmosphere and surface missions," in *Proc. 11th Int. Energy Convers. Eng. Conf.*, 2013, [Online]. Available: https://arc.aiaa.org/doi/abs/10.2514/6.2013-4028

[3] E. E. Perl *et al.*, "(Al)GaInP/GaAs tandem solar cells for power conversion at elevated temperature and high concentration," *IEEE J. Photovolt.*, vol. 8, no. 2, pp. 640–645, Mar. 2018.

[4] V. I. Moroz *et al.*, "Spectrum of the Venus day sky," *Nature*, vol. 284, pp. 243–244, 1980.

[5] D. V. Titov *et al.*, "Radiation in the atmosphere of Venus," in *Exploring Venus as a Terrestrial Planet* (Geophysical Monograph Series 176), L. W. Esposito, E. R. Stofan, and T. E. Cravens, Eds., Washington, DC, USA: American Geophysical Union, 2013, pp. 121–138.

[6] D. M. Hunten, L. Colin, T. M. Donahue, and V. I. Moroz, *Venus*, 1983, [Online]. Available: https://uapress.arizona.edu/book/venus

[7] A. P. Ekonomov *et al.*, "Scattered UV solar radiation within the clouds of Venus," *Nature*, vol. 307, pp. 345–347, 1984.

[8] V. I. Moroz *et al.*, "Solar and thermal radiation in the Venus atmosphere," *Adv. Space Res.*, vol. 5, pp. 197–232, 1985.

[9] Y. Sun et al., "Thermal stability of GaAs solar cells for high temperature applications," in *Proc. IEEE 43rd Photovolt. Specialists Conf.*, 2016, pp. 2385–2388.

[10] G. A. Landis, D. J. Belgiovane, and D. A. Scheiman, "Temperature coefficient of multijunction space solar cells as a function of concentration," in *Proc. 37th IEEE Photovolt. Specialists Conf.*, 2011, pp. 001583–001588.

[11] P. Singh and N. M. Ravindra, "Temperature dependence of solar cell performance—An analysis," *Solar Energy Mater. Solar Cells*, vol. 101, pp. 36–45, 2012.

[12] J. D. Cressler and H. A. Mantooth, *Extreme Environment Electronics*. Boca Raton, FL, USA: CRC Press, 2012, [Online]. Available: https://www.crcpress.com/Extreme-Environment-Electronics/Cressler-Mantooth/p/book/9781138074224

[13] B. Welber, M. Cardona, C. K. Kim, and S. Rodriguez, "Dependence of the direct energy gap of GaAs on hydrostatic pressure," *Phys. Rev. B*, vol. 12, pp. 5729–5738, 1975.

[14] I. Garcia, I. Rey-Stolle, C. Algora, W. Stolz, and K. Volz, "Influence of GaInP ordering on the electronic quality of concentrator solar cells," *J. Cryst. Growth*, vol. 310, pp. 5209–5213, 2008.

[15] J. Grandidier, D. M. Callahan, J. N. Munday, and H. A. Atwater, "Light absorption enhancement in thin-film solar cells using whispering gallery modes in dielectric nanospheres," *Adv. Mater.*, vol. 23, pp. 1272–1276, 2011.

[16] J. Grandidier, D. M. Callahan, J. N. Munday, and H. A. Atwater, "Gallium arsenide solar cell absorption enhancement using whispering gallery modes of dielectric nanospheres," *IEEE J. Photovolt.*, vol. 2, no. 2, pp. 123–128, Apr. 2012.

[17] L. A. A. Bunthof, J. Bos-Coenraad, W. H. M. Corbeek, E. Vlieg, and J. J. Schermer, "The illumination angle dependency of CPV solar cell electrical performance," *Solar Energy*, vol. 144, pp. 166–174, 2017.

[18] M. G. Tomasko, L. R. Doose, P. H. Smith, and A. P. Odell, "Measurements of the flux of sunlight in the atmosphere of Venus," *J. Geophys. Res.: Space Phys.*, vol. 85, pp. 8167–8186, 1980.

[19] J. Cutts et al., "Venus surface sample return—Role of balloon technology," in *Proc. AIAA Int. Balloon Technol. Conf.*, 1999, [Online]. Available: https://arc.aiaa.org/doi/abs/10.2514/6.1999-3855

[20] S. R. Johnson and T. Tiedje, "Temperature dependence of the Urbach edge in GaAs," *J. Appl. Phys.*, vol. 78, pp. 5609–5613, 1995.

[21] R. T. Lee *et al.*, "Enhancement of compositional modulation in GaInP epilayers by the addition of surfactants during organometallic vapor phase epitaxy growth," *J. Cryst. Growth*, vol. 233, pp. 490–502, 2001.

[22] S. Tomasulo, J. Simon, P. J. Simmonds, J. Biagiotti, and M. L. Lee, "Molecular beam epitaxy of metamorphic $In_yGa_{1-y}P$ solar cells on mixed anion $GaAs_xP_{1-x}$/GaAs graded buffers," *J. Vacuum Sci. Technol. B*, vol. 29, p. 03C118, 2011.

[23] P. Yeh and M. Hendry, "Optical waves in layered media," *Phys. Today*, vol. 43, p. 416, Mar. 2005, [Online]. Available: https://www.wiley.com/en-us/Optical+Waves+in+Layered+Media-p-9780471731924

[24] E. Anemogiannis, E. N. Glytsis, and T. K. Gaylord, "Determination of guided and leaky modes in lossless and lossy planar multilayer optical waveguides: Reflection pole method and wavevector density method," *J. Lightwave Technol.*, vol. 17, no. 5, pp. 929–941, May 1999.

Authors' photographs and biographies not available at the time of publication.